Supporting Information

Low-threshold Colloidal Quantum Dots Polariton Lasing via a Strong Coupling Microcavity at Room Temperature

Junxing Dong[1], Yuting Wu[2], Runchen Wang[1], Lisheng Wang[1], Jingzhuo Wang[1], Yifan Zhang[1], Yue Wang[2*], Xianghu Wang[3], Si Shen[4*] and Hai Zhu[1*]

[1]State Key Laboratory of Optoelectronic Materials and Technologies, School of Physics, Sun Yat-Sen University, Guangzhou 510275, China

[2]College of Materials Science and Engineering, Nanjing University of Science and Technology, Nanjing 210094, China

[3]School of Materials, Shanghai Dianji University, Shanghai 200245, China

[4]East China Normal University, Shanghai, 200241, China

*E-mail: ywang@njust.edu.cn, sshen@lps.ecnu.edu.cn, zhuhai5@mail.sysu.edu.cn

1. Details of the chemicals and the preparation of the precursor

Chemicals: Cadmium oxide (CdO, 99.9%), zinc acetate ($Zn(Ac)_2$, 99.99 %), oleic acid (OA, 90%), decanoic acid (98%), 1-octadecene (ODE, 90%), selenium powder (Se, 99.99%), tri-n-octylphosphine (TOP, 97%) and sulfur powder (S, 99.99%). All materials were used as received.

Zinc precursor: a mixture of $Zn(Ac)_2$ (5 mmol), OA (2 ml) and ODE (8 ml) was loaded into a 50 ml flask, heated to 130 °C and exhausted for 1h, followed by heating up to 240 °C and holding for 30 min. Selenium precursor: 1 mmol selenium powder was mixed with 2 ml TOP and stirred to obtain a clear solution. Sulfur precursor: 1 mmol selenium powder, 1 ml TOP and 4 ml ODE were mixed together, and stirred to get a clear solution.

2. Designs of the microcavity

Figure.S1a shows the reflectance spectrum of the DBRs structure used in the microcavity. The reflectance remains close to 1 in the range of 585-785 nm, to ensure confining light field within the microcavity. The scanning electron microscope (SEM) image shows the distribution morphology of CQDs that spin-coated on the DBRs template (**Figure.S1b**). The CQDs samples are evenly distributed, showing good spatial consistency.

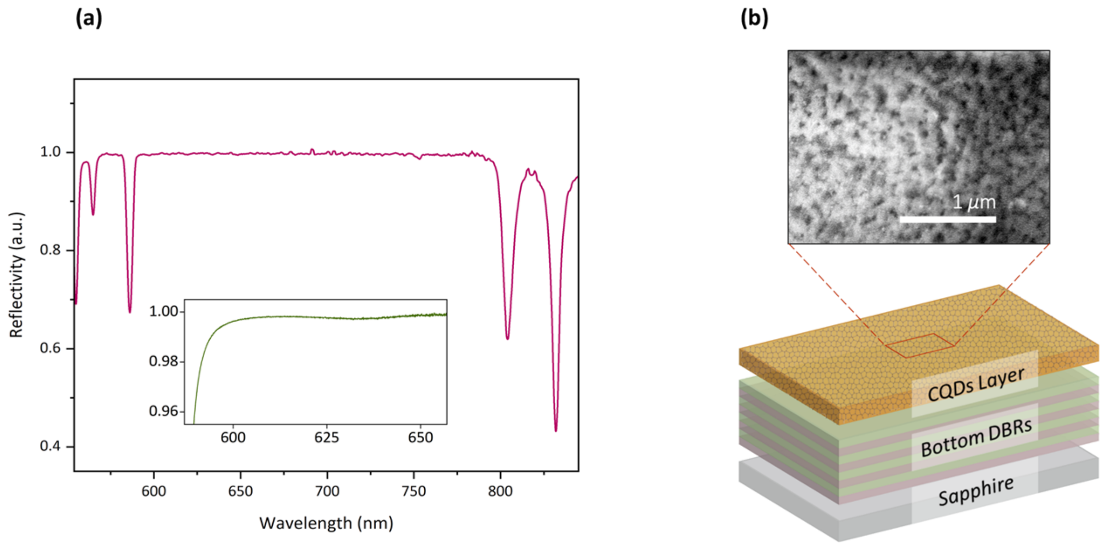

Figure S1. (**a**) Reflectance spectrum of the DBRs structure. (**b**) SEM image of the CQDs spin-coated on the DBRs surface.

3. Descriptions of the micro-photoluminescence setup

The schematic diagram of the angle-resolved micro-photoluminescence system is shown in **Figure S2**. The laser emitted from the regenerative amplification system passes through a BBO crystal for frequency doubling and then pumps the sample and collects signals through the co-focusing of two objective lenses (1, 2). A $4f$ system composed of two lenses (1, 2) is used after the collection objective lens, and the energy-momentum dispersion relationship is imaged on the two-dimensional array of the spectrometer's CCD. By adding a pinhole for spatial filtering at the real plane between the two lenses, this system can achieve micrometer-level spatial resolution. In an additional optical path, a lens (Len3) confocal with Len1 and a Michelson interferometer path are added to detect the coherence of the signal. The TCSPC module is added at the end of the collection path.

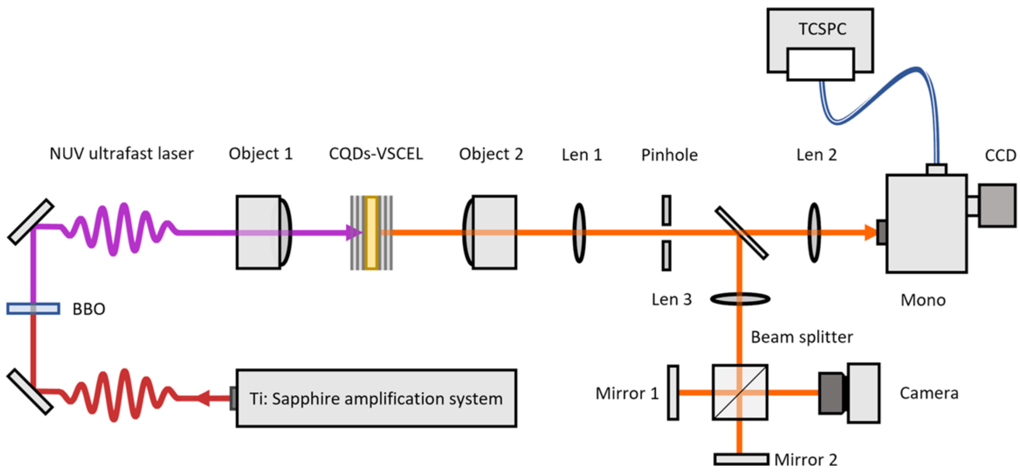

Figure S2. Schematic of the angle-resolved micro-photoluminescence system

4. Descriptions of strong-coupled system in planar microcavity

The planar microcavity only restricts the vibration modes of the optical field in the direction perpendicular to the microcavity. If the wavevector k of the optical field is decomposed into perpendicular component $k_\perp$ and parallel component $k_\parallel$, the dispersion relation of the cavity modes can be written as [12]

$$E_C(k_{||}) = \frac{\hbar c}{n_C} k = \frac{\hbar c}{n_C} \sqrt{k_\perp^2 + k_{||}^2} \#(1)$$

where n_c is the refractive index of the cavity medium. For the small-angle dispersion region where $k_\parallel \ll k_\perp$, the above equation can be approximated as follows:

$$E_C(k_{||}) = \frac{\hbar c}{n_C} k_\perp \sqrt{1 + k_{||}^2 / k_\perp^2} \approx \frac{\hbar c}{n_C} k_\perp \left(1 + \frac{k_{||}^2}{2k_\perp^2}\right) \#(2)$$

Thus, the dispersion behavior of the cavity mode $k_\parallel$ is approximately parabolic, and the effective mass of the cavity mode photon m_c is given by

$$m_C = \frac{\hbar n_C k_\perp}{c} = \frac{h n_C^2}{c \lambda_0} \#(3)$$

where λ_0 is the vacuum wavelength of the cavity mode at $k_\parallel = 0$, and c is the speed of light in vacuum.

The confinement effect of the microcavity on the optical field can enhance the coupling strength between excitons in the semiconductor gain material and cavity mode photons, bringing the system into the strong coupling regime. The eigenstates of the system transform into exciton-polariton states.[3] The Hamiltonian of the system can be written as the sum of the photon term, the exciton term, and the interaction term:

$$H = \sum_k E_C(k) a_k^\dagger a_k + \sum_k E_X(k) b_k^\dagger b_k + \sum_k \hbar\Omega\left(a_k^\dagger b_k + b_k^\dagger a_k\right) \# (4)$$

where a_k and b_k are the annihilation operators for photons and excitons at wavevector k, respectively, and $\hbar\Omega$ is the dipole interaction strength between excitons and photons. By using a_k and b_k, two new operators can be constructed: $l_k = C_k a_k + X_k b_k$, $u_k = X_k a_k - C_k b_k$, and the normalization condition: $|X_k|^2 + |C_k|^2 = 1$. If we set

$$|X_k|^2 = \frac{1}{2}\left[1 + \frac{\Delta E(k)}{\sqrt{\Delta E(k)^2 + 4\hbar^2\Omega^2}}\right] \# (5)$$

$$|C_k|^2 = \frac{1}{2}\left[1 - \frac{\Delta E(k)}{\sqrt{\Delta E(k)^2 + 4\hbar^2\Omega^2}}\right] \# (6)$$

where $\Delta E(k) = E_C(k) - E_X(k)$, the Hamiltonian of the system can be diagonalized as

$$H = \sum_k E_{LP}(k) l_k^\dagger l_k + \sum_k E_{UP}(k) u_k^\dagger u_k \# (7)$$

The new operators $\left(l_k^\dagger, l_k\right)$ and $\left(u_k^\dagger, u_k\right)$ describe two new eigenstates of the system. $|X_k|^2$ and $|C_k|^2$ define the photon and exciton component ratios of the upper and lower energy branches, respectively, known as Hopfield coefficients. Considering a real system, with the cavity mode loss rate γ_C and the exciton nonradiative relaxation rate γ_X, the dispersion of exciton-polariton can be written as

$$E_{LP}(k) = \frac{1}{2}[E_C + E_X + i(\gamma_C + \gamma_X) - \sqrt{[E_C - E_X + i(\gamma_C - \gamma_X)]^2 + 4\hbar^2\Omega^2}] \# (8)$$

$$E_{UP}(k) = \frac{1}{2}[E_C + E_X + i(\gamma_C + \gamma_X) + \sqrt{[E_C - E_X + i(\gamma_C - \gamma_X)]^2 + 4\hbar^2\Omega^2}] \# (9)$$

The strong coupling condition in a dissipative system is: $2\hbar\Omega \geq \gamma_X + \gamma_C$. As the density of polaritons increases, the system can be well explained by the Bose-Einstein distribution. When the average distance between particles is comparable to the de Broglie wavelength, the particles can become correlated through the overlap of their de Broglie waves, forming a coherent state with a unified phase. This corresponds to a significant increase in the occupancy of polaritons in the ground state $(k_{\parallel} = 0)$. That is:

$$\lambda_{th} = \frac{h}{\sqrt{2\pi m k_B T}} \approx r_s = n^{-1/2} \#(10)$$

According to Yamamoto assumption[4], the interaction strength g between polaritons is given as

$$g \approx 6E_b a_B^2 \#(11)$$

where E_b is excitonic binding energy and a_B is the excitonic Bohr radius. Based on mean-field approximation, the blue shift of ground state energy is approximately linear with the polariton density in low particle density regime, that is:

$$\Delta E = gn \#(11)$$

References

1. Babic D. I. et al. Analytic expressions for the reflection delay, penetration depth, and absorptance of quarter-wave dielectric mirrors. *IEEE J. of Quantum Electronics* 28, 514–524 (1992).
2. Panzarini G. et al. Quantum theory of exciton polaritons in cylindrical semiconductor microcavities. *Phys. Rev. B* 60, 16799–16806 (1999).
3. Deng H. et al. Exciton-polariton Bose-Einstein condensation. *Rev. Mod. Phys.* 82, 1489–1537 (2010).
4. Yamamoto, Y. et al. Exciton-exciton scattering dynamics in a semiconductor microcavity and stimulated scattering into polaritons. *Phys. Rev. B* 59, 10830–

10842 (1999).